Multi-Filter Photometric Analysis of Three β Lyrae-type Eclipsing Binary Stars

Tyler Gardner
Gage Hahs
Vayujeet Gokhale
Truman State University, Department of Physics, 100 E. Normal, Kirksville, MO 63501; gokhale@truman.edu

Received September 28, 2015; revised October 9, 2015; accepted November 24, 2015

Abstract We present light curve analysis of three variable stars, ASAS J105855+1722.2, NSVS 5066754, and NSVS 9091101. These objects are selected from a list of β Lyrae candidates published by Hoffman *et al.* (2008). Light curves are generated using data collected at the the 31-inch NURO telescope at the Lowell Observatory in Flagstaff, Arizona, in three filters: Bessell B, V, and R. Additional observations were made using the 14-inch Meade telescope at the Truman State Observatory in Kirksville, Missouri, using Baader R, G, and B filters. In this paper, we present the light curves for these three objects and generate a truncated eight-term Fourier fit to these light curves. We use the Fourier coefficients from this fit to confirm ASAS J105855+1722.2 and NSVS 5066754 as β Lyrae-type systems, and NSVS 9091101 to possibly be a RR Lyrae-type system. We measure the O'Connell effect observed in two of these systems (ASAS J105855+1722.2 and NSVS 5066754), and quantify this effect by calculating the "Light Curve Asymmetry" (LCA) and the "O'Connell Effect Ratio" (OER).

1. Introduction

Eclipsing binary systems are of particular importance to astronomy since they provide a unique opportunity to determine stellar parameters like the mass, radii, and luminosity of each component to a high degree of accuracy. Moreover, once the orbital period, inclination, and radial velocity of the system are determined, the radii of the stars can be determined. Of particular interest are β Lyrae-type systems which exhibit a continuous variation in the light curve, believed to be due to the tidal distortion of the individual components.

We selected three candidate β Lyrae-type systems from Hoffman *et al.* (2008) to determine the exact nature of these systems—whether they are Algols, W UMa-, or β Lyrae-type systems. This project is part of an effort at Truman State University (TSO) to introduce undergraduate students to differential aperture photometry by following three to four eclipsing binary systems per semester with the aim of generating light curves and modeling these systems. Apart from the primary objective of classifying these systems correctly, we are also interested in observing and studying the O'Connell effect (O'Connell 1951), which is the inequality in the out-of-phase maxima in the light curve of eclipsing binaries. The origin of this asymmetry is not well studied or understood, though the most common explanation for this phenomenon is the presence of star spots and/or a hot spot resulting from mass transfer between the components of the binary system (Koju and Beaky 2015).

In the following section, we outline our observational data acquisition and data reduction methods, followed by an analysis of the light curves in section 3. We conclude in section 4 with a discussion on our results and our future plans.

2. Observations

We present BVR photometry of eclipsing variable stars ASAS J105855+1722.2 (period P = 0.38 d), NSVS 5066754 (P = 0.375 d), and NSVS 9091101 (P = 0.25107 d). The data were collected using the 2k × 2k Loral NASACam CCD attached to the 31-inch NURO telescope at Lowell Observatory, Flagstaff, Arizona. The filters used are Bessell BVR. Additional data were obtained (see Table 1) using the SBIG STT-8300 CCD camera attached to the 14-inch LX-200 Meade telescope at the Truman State Observatory at Kirksville, Missouri. The filters used are Baader Planetarium RGB filters. The NURO images are processed by bias subtraction and (sky) flat fielding using the software package MAXIMDL (Diffraction Limited 2012). No dark subtraction was performed since for the nitrogen-cooled camera at NURO, the dark current is negligible. The TSO images are processed by bias and dark subtraction, and (dome) flat fielding using MAXIMDL. Differential photometry is then performed on the target with a suitable comparison and check star, using MAXIMDL and the AAVSO photometry tool VPHOT (Klingenberg and Henden 2013). The aperture size was adjusted to match between 3 to 4 times the full width at half maximum (FWHM) of the brightest object on which photometry was performed for a given target. Similarly, the inner sky annulus was adjusted to about 5 times the FWHM (Beck *et al.* 2015). We searched for any comparison stars from the Tycho (Høg *et al.* 2000) and APASS3 catalogues (Henden *et al.* 2012) that are present in the image frame, and used these stars to determine the B and V magnitudes

Table 1. Observation dates, instrument and filters for the targets.

Target	*Observation Date*	*Telescope*	*Filters*
ASAS J105855+1722.2	03/10/2015	NURO	Bessell BVR
	03/11/2015	NURO	Bessell BVR
	03/20/2015	TSO	Baader RGB
	03/21/2015	TSO	Baader RGB
NSVS 5066754	04/10/2015	TSO	Baader RGB
	10/25/2014	TSO	Baader RGB
	10/28/2014	TSO	Baader RGB
	10/29/2014	TSO	Baader RGB
NSVS 9091101	10/31/2014	TSO	Baader RGB
	11/01/2014	TSO	Baader RGB
	11/24/2014	NURO	Bessell BVR
	11/26/2014	NURO	Bessell BVR

Table 2. Target, comparison, and check star coordinates and comparison star B and V magnitudes.

Star Designation	*Position* R.A. (2000) h m s	Dec. (2000) ° ′ ″	*V*	*B*
Target Stars				
ASAS J105855+1722.2	10 58 55.05	+17 22 12.1	—	—
NSVS 5066754	13 20 57.77	+47 29 29.3	—	—
NSVS 9091101	00 22 43.44	+08 50 05.9	—	—
Comparison Stars				
TYC 1429-165-1	10 58 57.953	+17 25 35.26	12.47	12.30
—	13 20 20.77	+47 33 42.2	12.541	13.388
—	00 22 16.12	+08 47 06.7	13.084	14.179
Check Stars				
—	10 59 01	+17 18 39.97	—	—
—	13 20 51	+47 25 46	—	—
—	00 22 45.9	+08 52 15.43	—	—

of each of the targets. Since we could not find the R magnitude of any of the comparison stars, differential photometry was performed on the R-filter data using instrumental magnitudes. Stars of brightness comparable to the target star were chosen as check stars. Please see Table 2 for details.

3. Analysis and results

For plotting the light curve for each object, the time axis is phase-folded using the period provided by Hoffman *et al.* (2008) and calculating the phase using the equation

$$\Phi = \frac{T - T_0}{P} - \text{Int}\left(\frac{T - T_0}{P}\right), \quad (1)$$

where P is the period of the system and T_0 is an arbitrarily chosen epoch. The resulting light curve in B and V for each object is shown in Figures 1, 2, and 3. The color B–V is plotted on the bottom panel of each light curve. It is clear from the light curves that ASAS J105855+1722.2 and NSVS 5066754 show two unequal eclipses, whilst only one eclipse is seen in NSVS 9091011. For each object we calculate the average B and V magnitude, and hence the average value of B–V. These values are tabulated in Table 3. Since we have used standard Johnson filters for ASAS J105855+1722.2 and NSVS 9091101, we use the B–V color to calculate an estimate of the temperature using Flower (1996). Unfortunately, we do not have the data to calculate the same for NSVS 5066754 or the NSVS 9091101 data collected at TSO. Nevertheless, the B–V plots for NSVS 5066754 and NSVS 9091011 appear to be more or less flat, which might indicate that the surface temperatures of the two components of the binary are similar. For ASAS J105855+1722.2, a slight "bump" can be seen around the secondary eclipse with a corresponding "dip" around the primary eclipse, which suggests that the hotter star is being eclipsed at primary eclipse, and the cooler component is

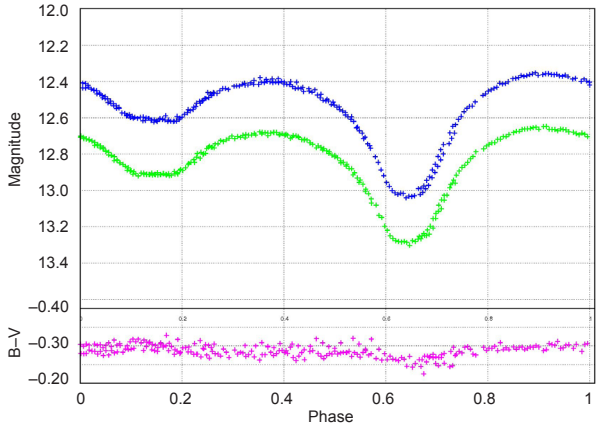

Figure 1. Light curve for ASAS J105855+1722.2, along with the B–V color versus orbital phase. The two colors denote Bessell B and V filters. Note the difference in depth of the two eclipses and the smoothly varying light curve. Also note the difference in the primary and secondary maxima (O'Connell effect).

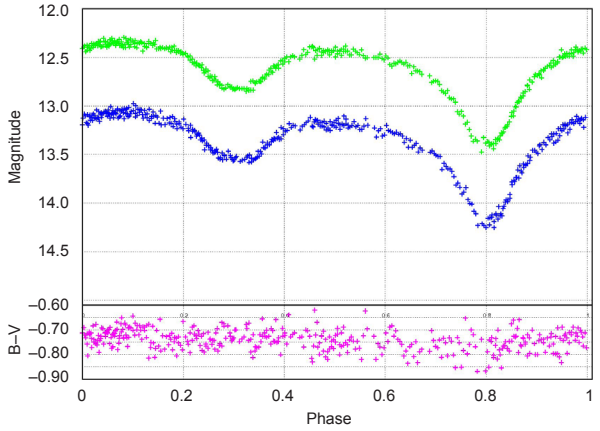

Figure 2. Light curve for NSVS 5066754 in Baader Blue and Green filters and the B–V color versus orbital phase. Note the difference in depth of the two eclipses and the smoothly varying light curve. Also note the difference in the primary and secondary maxima (O'Connell effect).

Table 3. Average B and V magnitudes, B–V color and Temperature estimate.

Target	*Average B*	*Average V*	*Average B–V*	*Temperature K*
ASAS J105855+1722.2	12.563	12.850	–0.287	30789
NSVS 5066754 (Baader filters)	13.349	12.607	0.742	—
NSVS 9091101 (Baader filters)	13.168	12.269	0.899	—
NSVS 9091101	13.008	12.241	0.767	5360

Note: The Baader filter values are "non-standard" and are shown here for completeness.

eclipsed at secondary eclipse. The color temperature of ASAS J105855+1722.2 is quite high, indicating the presence of early-type components.

We converted the differential magnitude measured in each filter to the normalized flux (Warner 2006) by using

$$I(m(\phi)) = I_{max}\ 10^{-0.4 \times (m(\phi) - m(max))} \quad (2)$$

where m(ϕ) is the magnitude dependent upon phase, m(max) is the maximum magnitude, and the I_{max} value is set to one.

Following Wilsey and Beaky (2009), we perform a Fourier fit analysis on the light curves for each of the objects we studied in each filter. The Fourier coefficients are then used to classify each system as either a β Lyrae, Algol, or WUMa system; and to quantify the O'Connell effect. The Fourier fit is accomplished using VSTAR (Benn 2013) provided by the American Association of Variable Star Observers (AAVSO). The fits are generated after the data for each object were shifted so that the primary eclipse occurred at phase 0. The truncated Fourier fit is given by

$$m(\phi) = \sum_{n=0}^{8} a_n \cos(2\pi n(\phi - \theta)) + b_n \sin(2\pi n(\phi - \theta)) \qquad (3)$$

where a_n and b_n are the Fourier coefficients, ϕ is the phase, and θ is the phase offset to compensate for the unknown time of the maximum/minimum (Hoffman *et al.* 2009).

3.1. Classification of systems

The comparison of the second and fourth cosine coefficients, a_2 and a_4, yields an estimate on the degree of contact of the system (Rucinski 1997). We refer to Rucinski (1973) and Rucinski (1993) for a detailed description of the use of the Fourier coefficients in determining the orbital elements of contact binary stars. For our purposes it is sufficient to appreciate that the a_2 coefficient attempts to quantify the tidal proximity effect in detached systems, whilst a_4 attempts to account for the symmetrical deviations from the exact double cosine term caused by the eclipses. Thus, a_2 is a measure of the global distortion of the contact structure, whilst a_4 represents the more localized eclipse effects. Rucinski (1997) summarizes these effects in terms of the two Fourier coefficients as follows: if $a_4 > a_2(0.125 - a_2)$ then the system can be considered a β Lyrae candidate. Furthermore, if $a_4 < a_2(0.125 - a_2)$ then the system may be considered detached eclipsing binary or Algol. In addition, if $|a_4| < 0.02$, the objects could be either RR Lyr or W UMa variables with periods under 1.2 days (Hoffman *et al.* 2008, 2009). We evaluated these relationships for each of our objects and the results are recorded in Table 4.

It is clear from the results in Table 4 that ASAS J105855 +1722.2 and NSVS 5066754 are β Lyrae-type systems. This is consistent with the fact that the light curves for these objects in each filter is continuously varying; and that the depth of the primary and secondary minima are not similar. Note that the third object, NSVS 9091101, does not show a secondary minima at all and has $|a_4| < 0.02$. Since the object cannot be classified as a W UMa, we classify it as either a β Lyrae or an RR Lyrae system based on the criteria outlined above.

3.2. Quantifying the O'Connell effect

The O'Connell effect is the asymmetry in the heights of the

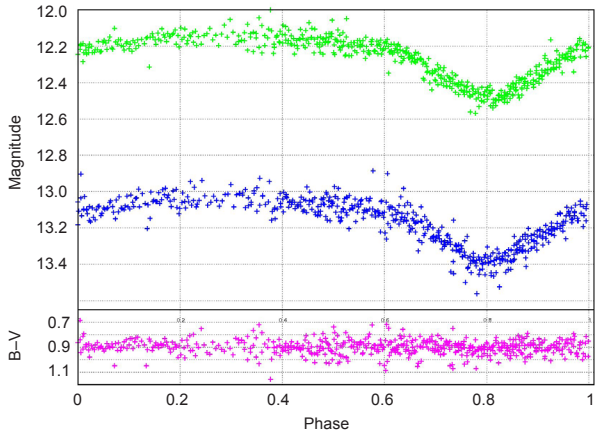

Figure 3. Light curve for NSVS 9091011 in Baader Blue and Green filters and the B–V color versus orbital phase. Note that the light curve varies smoothly, and only one eclipse is observed.

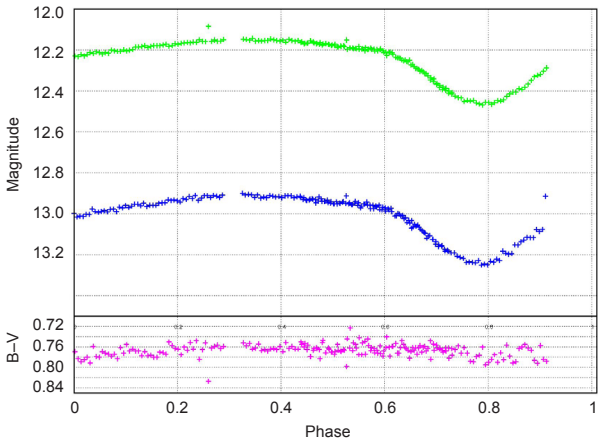

Figure 4. Light curve for NSVS 9091011 in Bessell B and V filters and the B–V color versus orbital phase. Note that the light curve varies smoothly, and only one eclipse is observed. Note that for this set of observations we do not have coverage over the entire phase.

Table 4. Classification of systems based on Fourier coefficients.

Target	*Filter*	a_2	a_4	$a_2(0.125 - a_2)$	*Classification*
ASAS J105855+1722.2	B	–0.15329	–0.03029	–0.04265907	β Lyr
	V	–0.15191	–0.03138	–0.04206368	β Lyr
	R	–0.15199	–0.03246	–0.04210057	β Lyr
NSVS 5066754	B	–0.18786	–0.05218	–0.05877538	β Lyr
	G	–0.19084	–0.05357	–0.06027592	β Lyr
	R	–0.19253	–0.05343	–0.06113507	β Lyr
NSVS 9091101	B	–0.01819	0.006372	–0.0026043	β Lyr/RR Lyr
	V	–0.0048	0.008484	–0.00062277	β Lyr/RR Lyr
	R	–0.01047	0.006927	–0.00141852	β Lyr/RR Lyr
NSVS 9091101 (TSO)	B	–0.038966	–0.005532	–0.0063891	β Lyr/RR Lyr
	G	–0.039086	–0.00707	–0.006413465	β Lyr/RR Lyr
	R	–0.038606	–0.00587	–0.006316173	β Lyr/RR Lyr

maxima observed in the light curves of some eclipsing binaries. A definite explanation for this phenomenon has been somewhat elusive, though the "starspot model" and the "hot spot model" have been suggested as possible explanations for the observed O'Connell effect (Koju and Beaky 2015). The simplest way to quantify the O'Connell effect is to calculate the difference between the primary (m_p) and secondary (m_s) maxima:

$$\Delta m = m_p - m_s \quad (4)$$

A positive Δm means the peak after the primary eclipse is brighter than the peak after the secondary eclipse. A negative Δm implies the opposite. By phase shifting our light curves such that the primary eclipse is set to phase θ = 0.0, we see that the peak magnitudes align approximately at phases θ = 0.25 and θ = 0.75, as shown in Figure 5 and Figure 6.

We use the coefficient of the first sine term in our Fourier fit to approximate Δm. The first sine term has extrema at phases θ = 0.25 and θ = 0.75. This makes it the dominant component accounting for the asymmetry in the peak magnitudes (Wilsey and Beaky 2009). In Figure 5 and Figure 6, we plot the first sine term with the light curve to show how the extremes of the sine wave align with the out-of-eclipse peak magnitudes. The coefficient, b_1, associated with the first sine term is the half-amplitude of the sine wave. This implies that $|2b_1|$ is a close approximation to Δm, and hence, a close approximation to the magnitude of the O'Connell effect. The $|2b_1|$ values for each of our objects are calculated from the Fourier coefficients and recorded in Table 5.

We calculated Δm in two other ways. Firstly, we found the values of the two peak magnitudes of the Fourier fit functions. The difference between the two maxima gives us a measure of the O'Connell effect. These values are presented in Table 5 as "Δm (Fourier)." Secondly, all of the data points within 0.05 phase of each maximum are averaged. The difference between the two average values for the maxima is calculated, yielding another measure of Δm. These values are recorded in Table 5 as "Δm (Average)."

Following Wilsey and Beaky (2009) and McCartney (1999), we quantified the O'Connell effect using two other

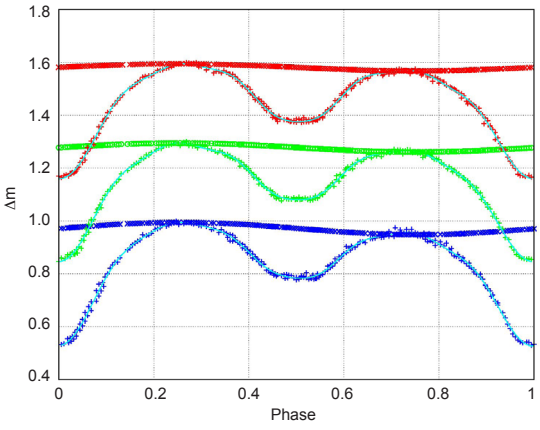

Figure 5. Differential magnitudes ("+" symbols) for ASAS J105855+1722.2. The Fourier fit (continuous curve) and the first sin term of the fit ("×" symbols) are plotted as well. The red, green, and blue curves correspond to RVB filters, respectively.

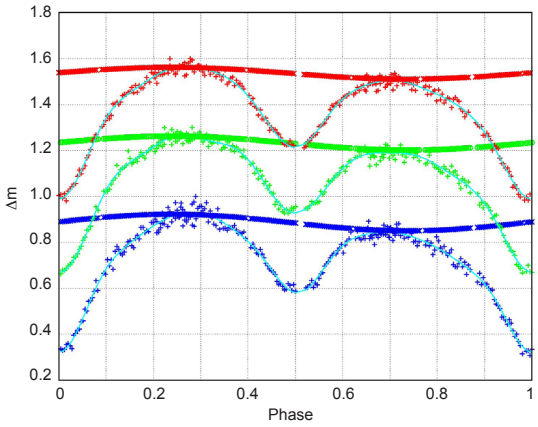

Figure 6. Differential magnitude ("+" symbols) for NSVS 5066754. The Fourier fit (continuous curve) and the first sin term of the fit ("×" symbols) are plotted as well. The red, green, and blue curves correspond to RGB filters, respectively.

Table 5. Quantifying the O'Connell effect in terms of difference in maxima. Please see the text (section 3.2) for details.

Target	*Filter*	$\|2b_1\|$	*Δm (Fourier)*	*Δm (Average)*
ASAS J105855+1722.2	B	0.047	0.037	0.036
	V	0.034	0.030	0.026
	R	0.026	0.027	0.026
NSVS 5066754	B	0.072	0.086	0.083
	G	0.060	0.077	0.070
	R	0.052	0.058	0.059

measures: the O'Connell Effect Ratio (OER) and the Light Curve Asymmetry (LCA). The OER and LCA provide insight into the asymmetries of the light curve regions between the two eclipses.

The OER is simply the ratio of the area under the curves for phases θ = 0.0 to θ = 0.5 and phases θ = 0.5 to θ = 1.0. An OER > 1 implies that the first half of the light curve has more total flux than the second half. There is strong correlation between the OER and Δm, as a positive Δm implies that the peak after the primary eclipse has more flux, which leads to an OER > 1. A negative Δm then implies an OER < 1. The LCA measures the deviance from symmetry of the two halves of the light curve. If both halves are perfectly symmetric, then we would expect the LCA to be zero. The LCA grows as the light curves become less symmetric. It is important to note that the LCA and OER quantify different aspects of the OC effect. For example, an OER equal to 1 does not necessarily imply an LCA equal to 0. The reason for this is that one can imagine a light curve with a tall but narrow peak maximum and short but wide secondary maximum. Although the areas under the curve of each region may be equal, the curves would be very asymmetric.

The Fourier fit (Equation 3) and the calculated relative flux (Equation 1) are used to determine the OER and LCA using

$$\mathrm{OER} = \frac{\int_{0.0}^{0.5} (I(\theta) - I(0.0))d\theta}{\int_{0.5}^{1.0} (I(\theta) - I(0.0))d\theta} \quad (5)$$

and,

$$LCA = \sqrt{\int_{0.0}^{0.5} \frac{(I(\theta) - I(1.0 - \theta))^2}{I(\theta)^2} d\theta} \quad (6)$$

The values for these parameters are tabulated in Table 6.

4. Discussion and future work

We have successfully completed the photometric light curve analysis of ASAS J105855+1722.2, NSVS 5066754, and NSVS 9091101. Based on our light curves and analysis we conclude that the first two systems are β Lyrae systems, while the third system is either a β Lyrae- or RR Lyrae-type system. None of these systems has shown any δ Scuti oscillations (Mkrtichian *et al.* 2004; Tempesti 1971) though the data collected at the Truman Observatory may be too noisy to ascertain any δ Scuti oscillations (which usually are in the millimagnitude range). Both ASAS J105855+1722.2 and NSVS 5066754 show a positive O'Connell effect.

We have tried to model these systems using photometric data alone, but we are not in a position to calculate a unique model. We are in the process of acquiring spectroscopic data (Powell 2015) in order to generate unique and accurate models for these systems. We are particularly interested in understanding the origin of the O'Connell effect based on these models in terms of the "starspot model" and the "hot spot model." To this end, we are in the process of quantifying the O'Connell effect in Kepler EBs using the Kepler Eclipsing Binary Catalogue maintained by Villinova University (Kirk *et al.* 2015). Additionally, we are in the process of acquiring photometric and spectroscopic data on low mass Kepler Eclipsing Binaries (Prša *et al.* 2011) which show the O'Connell effect in order to accurately model these systems and to determine the properties of hotspots and/or starspots (size, lifecycle and so on) in these systems. We believe that this information will be useful to discern the effects of these spots in the detection of exoplanets around low mass (single) stars.

5. Acknowledgements

The authors would like to thank W. Lee Powell for helpful discussions. We have made extensive use of the tools avaliable on the AAVSO website, in particular, the VSP tool to generate star charts, and the VSTAR and VPHOT tools to perform photometry. In addition, we have used the SIMBAD database, operated at CDS, Strasbourg, France and NASA's Astrophysics Data System. We are thankful for the support provided by the Office of Student Research at Truman State University, and to the Missouri Space Grant Consortium. This research was made possible through the use of the AAVSO Photometric All-Sky Survey (APASS), funded by the Robert Martin Ayers Sciences Fund. The authors would also like to thank the anonymous referee for useful comments and suggestions, which greatly improved the manuscript.

Table 6. Quantifying the O'Connell effect in terms of OER and LCA. Please see text (section 3.2) for the definitions of the OER and LCA.

Target	*Filter*	*OER*	*LCA*
ASAS J105855+1722.2	B	1.08629	0.024018
	V	1.06753	0.018802
	R	1.05793	0.014743
NSVS 5066754	B	1.14588	0.054379
	G	1.12555	0.044532
	R	1.11302	0.040538

References

Beck, S., Henden A., and Templeton, M. 2015, *The AAVSO Guide to CCD Photometry*, AAVSO, Cambridge, MA (https://www.aavso.org/ccd-photometry-guide).

Benn, D. 2013, VSTAR data analysis software (http://www.aavso.org/vstar-overview).

Diffraction Limited. 2012, MAXIMDL image processing software (http://www.cyanogen.com).

Flower, P. J. 1996, *Astrophys. J.*, **469**, 355.

Henden, A. A., Levine, S. E., Terrell, D., Smith, T. C., and Welch, D. L. 2012, *J. Amer. Assoc. Var. Star Obs.*, **40**, 430 (https://www.aavso.org/apass).

Hoffman, D. I., Harrison, T. E., Coughlin, J. L., McNamara, B. J., Holtzman, J. A., Taylor, G. E., and Vestrand, W. T. 2008, *Astron. J.*, **136**, 1067.

Hoffman, D. I., Harrison, T. E., and McNamara, B. J. 2009, *Astron. J.*, **138**, 466.

Høg, E., *et al.* 2000, *Astron. Astrophys.*, **355**, L27.

Kirk, J., *et al.* 2015, Kepler Eclipsing Binary Stars (Catalog V3; in preparation; http://keplerebs.villanova.edu/).

Klingenberg, G., and Henden, A. A. 2013 VPHOT photometric analysis tool (http://www.aavso.org/vphot).

Koju, V., and Beaky, M. 2015, *Inf. Bull. Var. Stars*, No. 6127, 1.

McCartney, S. A. 1999, Ph.D. dissertation, University of Oklahoma.

Mkrtichian, D. E., *et al.* 2004, *Astron. Astrophys.*, **419**, 1015.

O'Connell, D. J. K. 1951, *Publ. Riverview Coll. Obs.*, **2**, 85.

Powell, L. 2015, private communication.

Prša, A., *et al.* 2011, *Astron. J.*, **141**, 83.

Ruciński, S. M. 1973, *Acta Astron.*, **23**, 79.

Rucinski, S. M. 1993, *Publ. Astron. Soc. Pacific*, **105**, 1433.

Rucinski, S. M. 1997, *Astron. J.*, **113**, 407.

Tempesti, B. 1971, *Inf. Bull. Var. Stars*, No. 596, 1.

Warner, B. D. 2006, *A Practical Guide to Lightcurve Photometry and Analysis*, Springer-Verlag, New York.

Wilsey, N. J., and Beaky M. M. 2009, in *The Society for Astronomical Sciences 28th Annual Symposium on Telescope Science. Held May 19–21, 2009 at Big Bear Lake, CA, Society for Astronomical Sciences, Rancho Cucamonga, CA, 107.*